Perovskite-derived structure modulation in the iron sulfate family†

Received 00th January 20xx,
Accepted 00th January 20xx

DOI: 10.1039/x0xx00000x

Yuanqi Lan[a,b‡], Qi Yan[a,c‡], Xinyuan Zhang[d], Wenjiao Yao[a]*, Chenchen Wang[e], Chun-sing Lee[e], Philip Lightfoot[f]*, Yongbing Tang,[a,b]*

We report the first example of a perovskite sulfate $[Na_3(H_2O)]Fe(SO_4)_3$. Further structure modulation, by dimensional reduction or ligand extension, has resulted in two related layered perovskite-like compounds $Na_6Fe(SO_4)_4$ and $Na_{12}Fe_3(SO_4)_6F_8$. Taken together, these results open up a more general strategy for the future design of more complex perovskite-related materials.

Perovskites, perhaps the most ubiquitous class of crystalline materials, are of great use in many fields, such as photonics, magnetism, ferroelectricity and superconductivity, thanks to their flexible compositions, diverse structures, and controllable physicochemical properties.[1-3] Conventionally, the perovskite family can be expressed by the generic composition ABX_3, where smaller transition metal ions on the B site reside in corner-sharing octahedra of X anions, and larger A-site cations have 12-fold coordination with X. With the intensive investigation on perovskites for several decades, the range of A, B and X have been expanded significantly, from transition metals to non-transition metals, from single-atom motifs to complex motifs, from inorganics to organics.[4-8] Examples of anions that may be incorporated at the perovskite-like X site include single-atom anions such as oxide or halide, and complex anions such as cyanide, formate, phosphate, oxalate, azide, tetrahydroborate and hypophosphite.[9-13] Regardless of the enormous range of perovskite variants, no sulfate member has been recognised to the best of our knowledge.

Meanwhile, structure modulation has been widely pursued for various applications. Among them, channel (including hollow, nanoporous) structures are promising for electrochromic devices, molecular sensors, molecular filters, hydrogen storage, etc.[14-16] A typical example is the application of Prussian blue analogues such as $Na_xCo[Fe(CN)_6]$ in storing cations in rechargeable batteries,[17-19] where the X in ABX_3-type perovskite is altered to CN^- so that the $[BX_3]$ cages are expanded by 35.6% based on edge length, to allow the migration of bigger A-site ions. Following this trend, the replacement of CN^- by even larger complex anions such as $[SO_4]^{2-}$ will further expand the $[BX_3]$ cages and lead to new materials suitable for various applications.

According to the above motivations, we have performed an intensive exploration in the iron sulfate system, and identified the first perovskite sulfate $[Na_3(H_2O)]Fe(SO_4)_3$ (***I***), in which the edge of the BX_3 cages is expanded by approximately 63.0% and 20.2% compared to $CaFeO_3$ and $Na_xCo[Fe(CN)_6]$, respectively. Moreover, by tailoring the structure of ***I***, two further layered derivatives, $Na_6Fe(SO_4)_4$ (***II***) and $Na_{12}Fe_3(SO_4)_6F_8$ (***III***) have been obtained, exhibiting expanded channel structures with B-B distances up to 2.95 times of that in the conventional perovskite $CaFeO_3$. As a representative, the electrochemistry of ***I*** is tested preliminarily, revealing its feasibility in ion storage. This study demonstrates a successful structural modulation strategy, and adds unique new members to the broader perovskite family.

When acting as the X ligand in ABX_3 perovskites, the size and symmetry of the oxide, cyanide and sulfate anions differ from each other and influence the framework structure. The radius of each is estimated to be 1.32, 1.91, and 2.58 Å,[20-22] leading to increased edge length (d) and volume (V) of the BX_3 cages. As shown in Figure 1, the d and V are enlarged by 35.6% and 150% from $CaFeO_3$ to $Na_xCo[Fe(CN)_6]$, and further by around 20.2% and 73% when replacing X with $[SO_4]^{2-}$. The overall increment from $CaFeO_3$ to ***I*** is 63.0% and 330% for d and V, respectively. Such evolution of BX_3 cages results in different void space sizes. More specifically, the size of A-site ions is 1.48 and 1.53 Å in $CaFeO_3$ and $Na_xCo[Fe(CN)_6]$, respectively, while in ***I***, three Na^+ ions and one water molecule occupy the large interstitial space. Therefore, the structural formula of ***I*** can be written as $[Na_3(H_2O)][Fe(SO_4)_3]$. Meanwhile, the non-centrosymmetric A-site occupation also triggers the distortion of

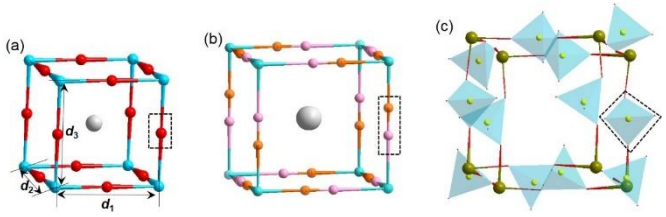

Fig. 1 Illustration of X size variation in the ABX_3 perovskite structure. (a) O ligand in $CaFeO_3$ with $d_1 = d_2 = d_3 = 3.896(7)$ Å, (b) CN ligand in $Na_xCo[Fe(CN)_6]$ with $d_1 = d_2 = d_3 = 5.285(5)$ Å, (c) SO_4 ligand in ***I*** with $d_1 = d_2 = 6.354(3)$ Å, $d_3 = 6.340(9)$ Å.

[a] *Advanced Energy Storage Technology Research Center, Shenzhen Institutes of Advanced Technology, Chinese Academy of Sciences, Shenzhen 518055, China. E-mail: wj.yao@siat.ac.cn; tangyb@siat.ac.cn*
[b] *Shenzhen College of Advanced Technology, University of Chinese Academy of Sciences, Shenzhen 518055, China.*
[c] *Nano Science and Technology Institute, University of Science and Technology of China, Suzhou, 215123, China.*
[d] *Tianjin Key Laboratory of Functional Crystal Materials, Institute of Functional Crystals, Tianjin University of Technology, Tianjin 300384, China.*
[e] *Center of Super - Diamond and Advanced Films and Department of Chemistry, City University of Hong Kong, Hong Kong SAR, 999077, P. R. China*
[f] *School of Chemistry and EaStChem, University of St Andrews, St Andrews, Fife, KY16 9ST, UK. E-mail: pl@st-andrews.ac.uk*

† Electronic Supplementary Information (ESI) available: Synthesis, crystallographic data (CIF), *etc*. CCDC 2031475 (**I**), 2050477 (**II**), 2099156 (**III**)

‡ These authors contributed equally to this work.

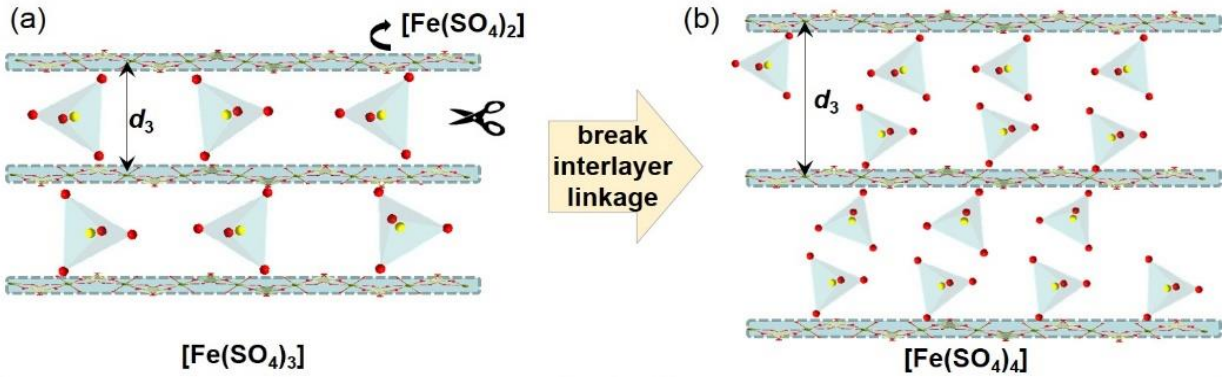

Fig. 2 Schematic illustration of breaking Fe[$(SO_4)_2$] interlayer linkage (indicated by scissors), leading to the transformation from ***I*** to ***II***. (a) The sulfate-linked layers in ***I***, (b) isolated layers in ***II,*** where $d_1 = d_2 = 6.198(6)$ Å, $d_3 = 9.684(3)$ Å.

the BX_3 cage. The B-B distances in ***I*** are identical in two directions but different in the third. More detailed representations of the true structure are given in Figure S1, Electronic Supplementary Information (ESI)

Next, following the development of conventional three-dimensional (3D) perovskite to two-dimensional (2D) layered perovskites, such as Ruddlesden-Popper phases,[23-25] we considered if such a structural modification is achievable in the perovskite sulfate family. Our strategy is schematically shown in Figure 2. In detail, based on the structure of ***I***, we aimed to break the nonidentical SO_4 linkage along the d_3 direction (same as d_3 in Figure 1) while maintaining the pseudo-planar [$Fe(SO_4)_2$] motif in the other two directions. By designing-in an extra SO_4 group the coordination around Fe remains six, but layering is achieved (i.e. the overall framework stoichiometry changes from [BX_3] to [BX_4]. Cations or molecules must lie in interlayer sites to keep the charge neutrality and structural stability. Under such considerations, a related layered sulfate with the formula $Na_6Fe(SO_4)_4$ (***II***) has been successfully obtained. We note that the generic formula can be represented as A_6BX_4, whereas the standard single-layered perovskite typically exhibit stoichiometries ABX_4 or A_2BX_4;[26-29] a significant increase in the extra-framework cation content is therefore permitted in this new family of layered perovskites.

The structure of ***II*** is shown schematically in Figure 2b. More detailed representations of the true structure are given in Figure S2, ESI. Here, we note that there are three distinct extra-framework Na^+ sites, and two distinct sulfate moieties, *viz.* 'in-plane' and 'apical'. From ***I*** to ***II***, the pseudo-planar [$Fe(SO_4)_2$] motif has been preserved, with a tiny shrinkage of the B-B length. However, due to the breaking of interlayer linkage, the layer-to-layer distance has been expanded from 6.340 Å in ***I*** to 9.684 Å in ***II***.

As structures with flexible channels or inter-layer spaces are highly desired in applications such as molecular sensors, gas separation, etc., we advanced this work by considering whether the pseudo-planar [$Fe(SO_4)_2$] layers in ***I*** and ***II*** can be further expanded so that the B-B distance within a layer be elongated. From single-atomic O to multi-atomic CN and SO_4 it is easy to imagine progressing from single polyhedral to multi-polyhedral linkers. The first choices might include bi-polyhedral groups such as pyrophosphate, pyrosulfate or pyroborate, etc. However, to keep the system as simple as possible, we started from making the best use of the existing components, *i.e.*, SO_4 and Fe, specifically by aiming to link two SO_4 tetrahedra through a further, bridging octahedral unit. Therefore, the task turns to finding a specific polyhedron that can bridge two SO_4 units. This requires four other mono-coordinated anions. Halides seem an obvious choice in this regard, therefore, we determined to incorporate fluorine into the system. After systematic modifications of synthesis conditions, $Na_{12}Fe_3(SO_4)_6F_8$ (***III***) was obtained, in which a triple polyhedral linker [$FeF_4(SO_4)_2$] was identified, as expected. It contains one FeF_4O_2 octahedron in the middle of two SO_4 tetrahedra (Figure 3b). The octahedron and tetrahedra are bonded together by sharing common O vertices, with fluoride ions terminal. Such linkers connect the B-site Fe, forming a pseudo-plane with the structural formula $Fe[FeF_4(SO_4)_2]_2$ (i.e. retaining the generic perovskite-like layer stoichiometry BX_2 where B= Fe, and X = $FeF_4(SO_4)_2$). Using this linker extension strategy, the B-B distance is enlarged from 6.196 Å in ***II*** to over 11 Å in ***III***, with an increment of 82%, and it is almost tripled when compared with our starting point, $CaFeO_3$ perovskite.

Meanwhile, the stacking of BX_2 layers in ***III*** may be compared to that in ***II***. In detail, the B-site iron's six-coordination environment is again completed by two extra, apical SO_4 groups lying below and above the layer. The difference is that the adjacent layers in ***II*** are exactly overlapped, while they are shifted along the BX_2 diagonal by half in ***III***, as illustrated in Figure 3c. This resembles the situation seen in the different families of more conventional layered perovskites, i.e., the Ruddlesden-Popper and Dion-Jacobson phases, for ***III*** and ***II***, respectively[30-33]. The actual motif is shown in Figure 3d, where it is clear that the vertex (Fe in B-site) of the upper layer (green shadow) lies right above the centre of the lower layer (blue shadow). Meanwhile, as the centre of the lower layer is void, the out-of-plane SO_4 groups suffer little steric hindrance or anion-anion repulsion from the adjacent layer. Therefore, the layer-to-layer distance is shortened significantly to 5.285 Å. In addition, the FeO_6 octahedra tilt all in one direction (Figure 3e). According to the Bond Valence Sum (BVS) method, the iron is in the +3 oxidation state for FeF_4O_2, and +2 for FeO_6 polyhedra.

It should be noted that the key aspects and similarities of the frameworks are hard to distinguish directly from the unit cell

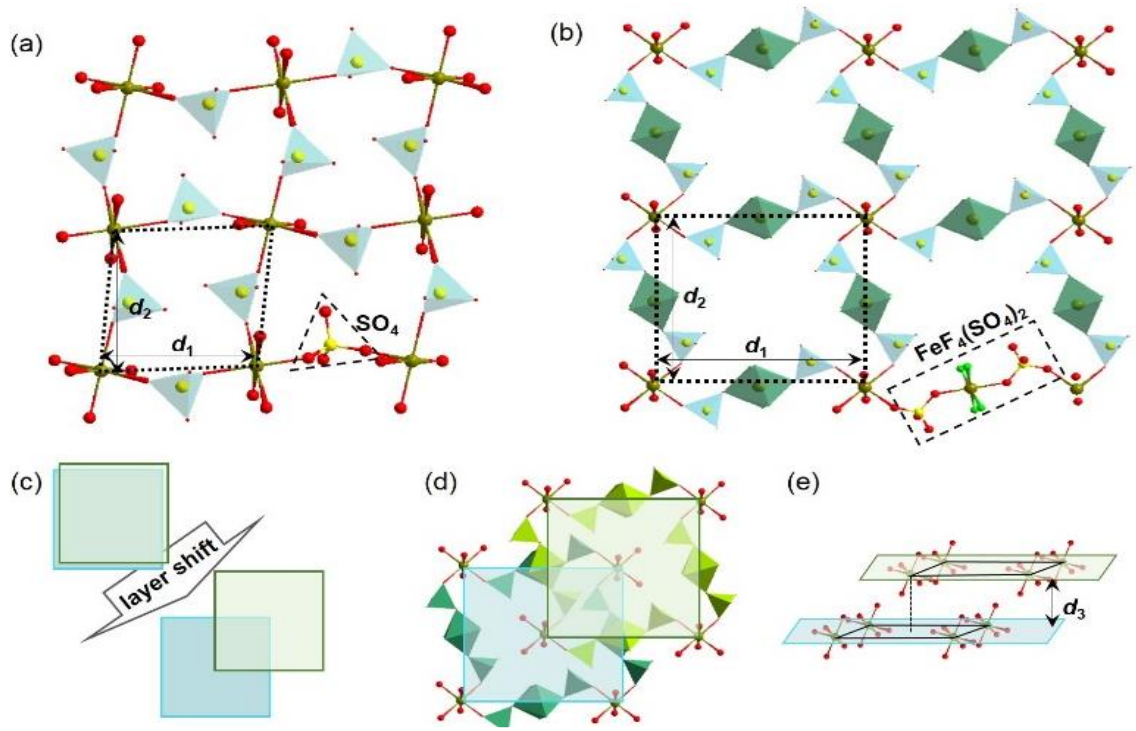

Fig. 3 Illustration of layer modulation by changing the X ligand from SO_4 in ***II*** (a) to $FeF_4(SO_4)_2$ in ***III*** (b). (c) Schematic illustration of the adjacent layer stacking pattern changes from overlapped in ***II*** to diagonally-shifted in ***III***. (d,e) Stacking layers in ***III*** from top (d) to side (e) views, in which the upper and bottom layers are in light green and blue, respectively. The corresponding distances are d_1 = 11.035(6) Å, d_2 = 11.532(4) Å, d_3 = 5.285(1) Å.

metrics. Further comparison of the crystal structures based on more conventional unit cell aspects are provided in Figure S1-2, ESI. As the structure evolves from ***I***, to ***II***, to ***III***, the complexity of the framework increases, the contained extra-framework spaces become larger, and the number of extra-framework cations increases, which compensate the void space and therefore the overall density. The detailed crystallographic data, crystal photos, powder X-ray diffraction patterns and spectroscopies of ***I***, ***II*** and ***III*** are displayed in Table S1-4 and Figure S3-6, ESI. Phase purity of each is confirmed by the PXRD. Interestingly, despite different local environments or iron's valence states, the FeX_6 octahedra are all in *trans*-mode, with only one symmetry element (Fe-site as centre of symmetry), and the bond lengths follow the sequence as Fe^{3+}-F<Fe^{3+}-O<Fe^{2+}-O (Figure S7, ESI).

As a representative of the possible physical properties of our new perovskite family, the electrochemistry of ***I*** was preliminarily tested. After stabilization, it exhibited two reversible redox reactions at, on average, 2.8 V and 3.2 V (Figure 4a). At 0.1 C (1 C = 80 mA g^{-1}), it de-inserts and inserts one Na-ion upon charge and discharge, respectively, corresponding to a stable capacity of ~ 80 mAh g^{-1}. As the rate increases, the capacity drops accordingly. The capacity at 1 C is about half of that at 0.1 C (Figure 4b). For the long cycle test, it is relatively stable for the attempted 200 cycles (Figure 4c). Therefore, it is revealed that the channels in ***I*** is suitable for Na-ion migration.

In summary, inspired by the well-known structural modulation from perovskite oxides, three sulfates exhibiting novel perovskite-like features have been derived. Among them, $[Na_3(H_2O)]Fe(SO_4)_3$ exhibits the first cubic perovskite-related structure in the sulfate family, where SO_4 occupies the X site in the ABX_3-type perovskite. Two strategies have been used to expand on this family of materials: first a 3D-to-2D structural design modification, mimicking the transition from perovskite to

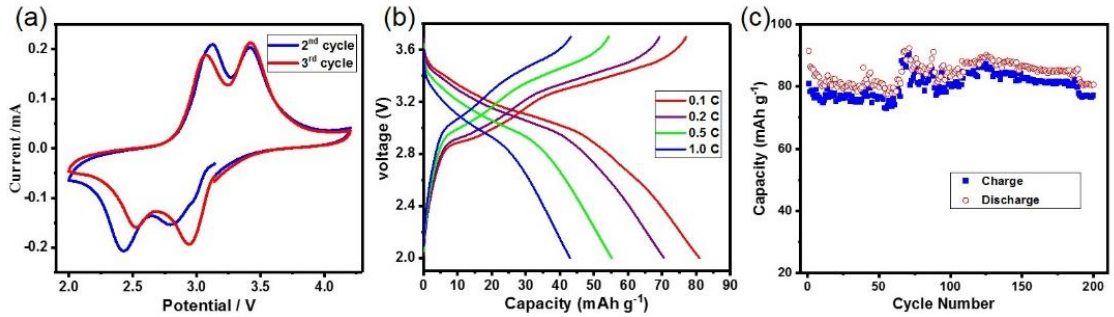

Fig. 4 Electrochemical properties of *I*. (a) Typical CV curve, (b) Charge-discharge curves, (c) Cycling performance at 0.2 C.

layered perovskite derivatives and, second, a ligand expansion strategy, specifically substitution of the SO_4 group by an extended polyanionic unit. These design principles have resulted in the identification of $Na_6Fe(SO_4)_4$ (***II***) and $Na_{12}Fe_3(SO_4)_6F_8$ (***III***) of which the resulting perovskite-like channel has been expanded up to 2.95 times of that in $CaFeO_3$. It should be noted that ***II*** is part of a wider family of previously reported compositions related to vanthoffite;[34] however, previous interpretations of these structures have never described them in the context of perovskite. Likewise, although ***III*** is a new compound, the manganese analogue has been reported.[35] Again, the structure type was not well understood in the original work, being described, perhaps incorrectly, as 'a 3D framework'; the relationship to layered perovskites was not apparent. The present descriptions and comparisons emphasise the importance of a thorough analysis and understanding of new structure types in order for them to be set within the context of existing work. Using an approach based on extrapolation and design, as in the present work, more sulfate-based perovskite-derived compounds can be expected, for example by coupling other inorganic or small organic ions as A-site cations, or replacing Fe with other transition metals as the B-site node, etc. The current study exemplifies a successful structural modulation strategy, opens up a novel perovskite-like family, whilst offering promising potential candidates for applications such as energy storage, gas filtering, contamination removal, and environmental remediation, etc.

We acknowledge support from Shenzhen Key Laboratory of Energy Materials for Carbon Neutrality (China). Thanks to Dr. Shu Guo from Southern University of Science and Technology (China), Dr. Yongping Zheng and Dr. Xiaolong Zhou from Shenzhen Institutes of Advanced Technology, Chinese Academy of Sciences (China) for helpful discussions. Thanks to support from National Natural Science Foundation of China (52125105, 22005329, 51972329, 52061160484), Shenzhen Science and Technology Planning Project (JCYJ20190807172001755, JCYJ20180507182512042), Science and Technology Planning Project of Guangdong Province (2019A1515110975, 2021A1515010184, 2019TX05L389), and Key-Area Research and Development Program of Guangdong Province (2019B090914003).

Conflicts of interest

There are no conflicts to declare.

Notes and references

1. J. Hwang, R. R. Rao, L. Giordano, Y. Katayama, Y. Yang and S. H. Yang, *Science*, 2017, **358**, 751-756.
2. L. T. Nguyen and R. J. Cava, *Chem. Rev.*, 2021, **121**, 2935-2965.
3. A. Simonov, T. De Baerdemaeker, H. L. B. Boström, M. L. Ríos Gómez, H. J. Gray, D. Chernyshov, A. Bosak, H.-B. Bürgi and A. L. Goodwin, *Nature*, 2020, **578**, 256-260.
4. H. L. B. Boström and A. L. Goodwin, *Acc. Chem. Res.*, 2021, **54**, 1288-1297.
5. H. L. Feng, C.-J. Kang, P. Manuel, F. Orlandi, Y. Su, J. Chen, Y. Tsujimoto, J. Hadermann, G. Kotliar, K. Yamaura, E. E. McCabe and M. Greenblatt, *Chem. Mater.*, 2021, **33**, 4188-4195.
6. L. G. Burley, A. K. Srivastava, S. Rudić and P. J. Saines, *Eur. J. Inorg. Chem.*, 2021, **2021**, 3806-3811.
7. R. Clulow, A. J. Bradford, S. L. Lee and P. Lightfoot, *Dalton Trans.*, 2019, **48**, 14461-14466.
8. L. Mao, W. Ke, L. Pedesseau, Y. Wu, C. Katan, J. Even, M. R. Wasielewski, C. C. Stoumpos and M. G. Kanatzidis, *J. Am. Chem. Soc.*, 2018, **140**, 3775-3783.
9. A. T. Giddings, E. A. S. Scott, M. C. Stennett, D. C. Apperley, C. Greaves, N. C. Hyatt and E. E. McCabe, *Inorg. Chem.*, 2021, **60**, 14105-14115.
10. D. B. Straus, S. Guo, A. M. Abeykoon and R. J. Cava, *Adv. Mater.*, 2020, **32**, 2001069.
11. L. G. Burley, J. H. Beecham-Lonsdale, A. K. Srivastava, I. E. Collings and P. J. Saines, *Dalton Trans.*, 2021, **50**, 5437-5441.
12. X. He, X. Zhang, B. Ji, W. Yao, P. Lightfoot and Y. Tang, *Chem. Commun.*, 2021, **57**, 2567-2570.
13. H. L. B. Boström, J. Bruckmoser and A. L. Goodwin, *J. Am. Chem. Soc.*, 2019, **141**, 17978-17982.
14. Y. Lan, W. Yao, X. He, T. Song and Y. Tang, *Angew. Chem. Int. Ed.*, 2020, **59**, 9255-9262.
15. B. Ji, W. Yao, Y. Zheng, P. Kidkhunthod, X. Zhou, S. Tunmee, S. Sattayaporn, H.-M. Cheng, H. He and Y. Tang, *Nat. Commun.*, 2020, **11**, 1225.
16. T. Song, W. Yao, P. Kiadkhunthod, Y. Zheng, N. Wu, X. Zhou, S. Tunmee, S. Sattayaporn and Y. Tang, *Angew. Chem. Int. Ed.*, 2020, **59**, 740-745.
17. Y. Moritomo, K. Igarashi, J. Kim and H. Tanaka, *Appl. Phys. Express*, 2009, **2**, 085001.
18. L. Deng, J. Qu, X. Niu, J. Liu, J. Zhang, Y. Hong, M. Feng, J. Wang, M. Hu, L. Zeng, Q. Zhang, L. Guo and Y. Zhu, *Nat. Commun.*, 2021, **12**, 2167.
19. H. L. B. Boström, I. E. Collings, D. Daisenberger, C. J. Ridley, N. P. Funnell and A. B. Cairns, *J. Am. Chem. Soc.*, 2021, **143**, 3544-3554.
20. J. Wasastjerna, *Comm Phys-Math, Soc. Sci. Fenn.*, 1923, **1**, 1-25.
21. H. D. B. Jenkins and K. P. Thakur, *J. Chem. Educ.*, 1979, **56**, 576.
22. Y. Marcus, *Chem. Rev.*, 1988, **88**, 1475-1498.
23. C. Fang, H. Wang and D. Li, *2D Mater.*, 2021, **8**, 022006.
24. C.-H. Li, M.-Y. Liao, C.-H. Chen and C.-C. Chueh, *J. Mater. Chem. C* , 2020, **8**, 4294-4302.
25. C.-R. Huang, X. Luo, X.-G. Chen, X.-J. Song, Z.-X. Zhang and R.-G. Xiong, *Natl. Sci. Rev.*, 2021, **8** (5), nwaa232.
26. D. M. Hatch, H. T. Stokes, K. S. Aleksandrov and S. V. Misyul, *Phys. Rev. B*, 1989, **39**, 9282-9288.
27. I. P. Swainson, *Acta Crystallogr. B* , 2005, **61**, 616-626.
28. K. J. Cordrey, M. Stanczyk, C. A. L. Dixon, K. S. Knight, J. Gardner, F. D. Morrison and P. Lightfoot, *Dalton Trans.*, 2015, **44**, 10673-10680.
29. Y.-Y. Guo, L.-J. Yang, S. Biberger, J. A. McNulty, T. Li, K. Schötz, F. Panzer and P. Lightfoot, *Inorg. Chem.*, 2020, **59**, 12858-12866.
30. V. A. Cascos, J. Roberts-Watts, C. Skingle, I. Levin, W. Zhang, P. S. Halasyamani, M. C. Stennett, N. C. Hyatt, E. Bousquet and E. E. McCabe, *Chem. Mater.*, 2020, **32**, 8700-8712.
31. J. A. McNulty and P. Lightfoot, *IUCrJ*, 2021, **8**, 485-513.
32. L. Mao, R. M. Kennard, B. Traore, W. Ke, C. Katan, J. Even, M. L. Chabinyc, C. C. Stoumpos and M. G. Kanatzidis, *Chem*, 2019, **5**, 2593-2604.
33. C. Han, A. J. Bradford, A. M. Z. Slawin, B. E. Bode, E. Fusco, S. L. Lee, C. C. Tang and P. Lightfoot, *Inorg. Chem.*, 2021, **60**, 11014-11024.
34. W. Fischer and E. Hellner, *Acta Cryst.*, 1964, **17**, 1613.
35. Q. Wang, A. Madsen, J. R. Owen and M. T. Weller, *Chem. Commun.*, 2013, **49**, 2121-2123.